

## Diffusion in curved fluid membranes

Nir S. Gov

*Department of Chemical Physics, The Weizmann Institute of Science, P.O. Box 26, Rehovot, Israel 76100*

(Received 22 April 2005; revised manuscript received 1 February 2006; published 14 April 2006)

We analyze theoretically the effects of curvature on the diffusion in a fluid membrane, within the Saffman-Delbrück hydrodynamic model. We calculate the effect of curvature on the *intrinsic fluidity* of a membrane through changes in its thickness, for both static or fluctuating curvature. We treat both thermal curvature fluctuations, and fluctuations due to active processes. Such curvature fluctuations increase the average membrane thickness and diminish the projected area, thereby decreasing the diffusion coefficient. This calculation allows us to predict the effect of shear flow on the membrane diffusion, and to compare to observations on living cells.

DOI: [10.1103/PhysRevE.73.041918](https://doi.org/10.1103/PhysRevE.73.041918)

PACS number(s): 87.16.Dg, 87.15.Vv, 05.40.-a, 61.30.St

### I. INTRODUCTION

In this paper we develop the theory of the diffusion of lipids and peptides in curved fluid membranes. The problem of diffusion in a flat membrane has been studied before using hydrodynamics [1] and free-area [2,3] approaches, and despite its fundamental importance in the context of biological cell membranes, has remained not fully resolved. We are concerned here with the effects of static and fluctuating membrane curvature on the diffusion coefficient, following the hydrodynamic approach of Saffman and Delbrück [1]. The effects of curvature on the diffusion have received very little theoretical consideration so far; in [4] the effect of curvature fluctuations on the diffusion was studied through the increase in the geometric path length which decreases the apparent (projected) diffusion.

A different effect of curvature, either static or fluctuating, which has not been treated so far, is the change in the *intrinsic membrane fluidity* through the induced changes in the membrane thickness [5,6]. Since most membranes in cells and vesicles are curved and support thermal and active curvature fluctuations (due to active membrane proteins or actin polymerization), the interplay between membrane curvature and diffusion is, therefore, of fundamental importance. A recent experimental study [7] which showed the effects of curvature in a monolayer on the diffusion coefficient has motivated the work presented here.

We begin with the model of Saffman and Delbrück [1] for the diffusion of a cylinder of length  $L$  and radius  $r$  in a membrane of width  $w$ , i.e., a two-dimensional fluid layer. We will deal here with a one component membrane, which is in its fluid phase. For simplicity we will treat here the case when  $L=w$ , where the solid cylinder represents either an inserted peptide (transmembrane protein) or a surfactant (or lipid) molecule. In this case of  $L=w$  the membrane is undeformed by the peptide. The drag force on the cylinder is proportional to its surface area, and by Einstein's relation the diffusion coefficient is [1]

$$D \approx \frac{k_B T}{2\pi w \eta} R_{log}, \quad (1)$$

where  $\eta$  is the internal viscosity of the membrane. The function  $R_{log}$  stands for logarithmic corrections that were calcu-

lated in [1]: One correction is of the form:  $R_{log} = \ln(\eta w / \eta_f a) - \gamma$ , where  $a$  is the radius of the diffusing object,  $\eta_f$  is the viscosity of the surrounding fluid, and  $\gamma$  is Euler's constant. Another correction is of the form:  $R_{log} = \ln(R/a) - \frac{1}{2}$ , where  $R$  is the lateral extent of a finite-size membrane. This correction is somewhat relevant to the case of diffusion in cylindrical membranes [7], where the flow is limited in the circumferential direction. This correction is significant when the radius of the cylindrical membrane is of the order of the inclusion radius or smaller. In the present experiments [7] this regime is never reached, with  $R/a \geq 20$ . We shall treat here only infinitely large membranes.

The effect of membrane curvature on the diffusion coefficient (1) can be included most simply through the curvature-induced changes to the membrane thickness  $w$ . When a monolayer is bent, its thickness increases or decreases, so as to maintain constant volume per surfactant (or lipid) molecules [5,6]. The calculation is done assuming pure curvature deformations, i.e., no overall compression or expansion of the membrane and a constant area per molecule at the neutral surface, and the molecular volume is kept constant. The symmetry between the hydrophilic and hydrophobic surfaces is broken by the strong head-group interactions which act to maintain a roughly constant area per head group. Such interactions are absent at the ends of the hydrophobic tails, and result in curvature-dependent membrane thickness [5,6]. For a monolayer or bilayer which are not under strong externally applied tensions, these assumptions are reasonable. They are also supported by some more detailed models, such as [8,9].

These calculations [5,6] assume that we are dealing with membranes that are weakly curved, such that the hydrodynamic calculation of Eq. (1) is valid. For static curvatures it means that we are always in the limit  $R/a \gg 1$  and  $R/w \gg 1$ . For fluctuating membranes we will work in the usual limit of small deformations away from the flat shape [5].

We note that there are other approaches to describe the diffusion inside fluid membranes, most notably the free-area model by Cohen and Turnbull [2,3]. This model proposes to take into account the discreteness of the lipid bilayers and describes a "jumping" movement of the molecules due to local packing defects. Comparison of this model to experi-

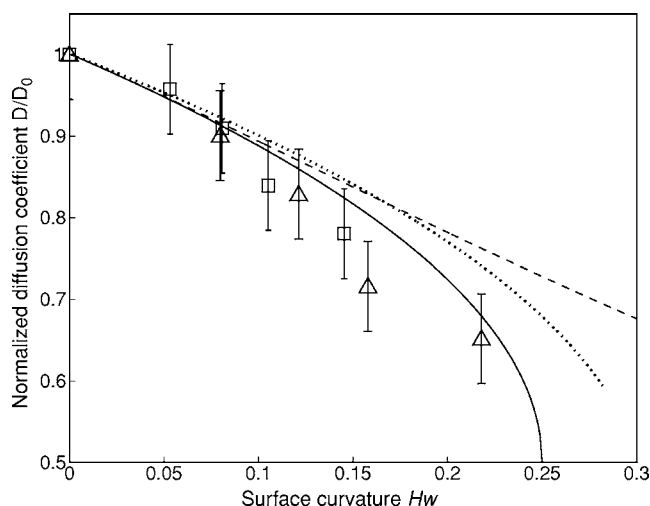


FIG. 1. The calculated dependence of the normalized diffusion coefficient  $D$  on the normalized mean membrane curvature  $Hw$  [Eq. (1)]; solid line, Eq. (3); dashed line, Eq. (2), compared to the experimental data [7]; squares, C18; triangles, C12. The dotted line is the solution for membrane thickness with a constant Gaussian curvature  $K=0.08$ , normalized by the unit membrane thickness.

ments has been rather difficult [10], but it has a clear potential advantage over the continuum model studied here by including specifically the microscopic details of the membrane structure.

The paper begins with the case of a static curvature (Sec. II), which we compare to recent experiments [7]. After we establish good agreement between our model and the experiments for the static case, we proceed to the case of a thermally fluctuating flat membrane (Sec. III) and fluctuating active membranes (Sec. IV). We then describe the effects of shear flow on cell membranes (Sec. V) and conclude in Sec. VI.

## II. STATIC CURVATURE

The mean and Gaussian curvatures ( $H$  and  $K$ ) have to be determined for any specific geometry, for the membrane thickness to be computed [5,6]. For a cylindrical geometry or undulations of a flat membrane, the Gaussian curvature is zero. If we set the Gaussian curvature to zero ( $K=0$ ) after expanding in the limit of small curvatures, the result is given by [5]

$$w_{eff,1} \approx w(1 - wH + 2w^2H^2). \quad (2)$$

Alternatively, we can set the Gaussian curvature to zero from the beginning, and get exactly

$$w_{eff,2} = \frac{-1 + \sqrt{1 + 4Hw}}{2H}. \quad (3)$$

Using both expressions (2) and (3) in Eq. (1), for a static negative  $H$ , the diffusion decreases with the curvature-induced increase in the membrane thickness. In Fig. 1 we show the theoretical curve along with the experimental measurements. The data are from very recent experiments [7],

which measured the diffusion of a fluorescent surfactant probe in an inverse-hexagonal phase, i.e., a surfactant monolayer in a cylindrical geometry. The data for the two types of surfactant probes were normalized by their respective bare thickness  $w$ , in the ratio of their chain lengths: 8 and 12 Å for the C12 and C18 probes, respectively. As predicted by our model, the experimental data, normalized by the thickness  $w$ , collapse on a single curve. In particular, the linear relationship for small curvatures shows the importance of the term which is linear in  $H$  in Eq. (2) for static curvatures. This is in contrast with the case of a fluctuating flat membrane, as discussed below.

The good agreement we find gives support to our picture of the curvature effects on the diffusion: The basic mechanism of molecular friction inside the monolayer is assumed not to change in any crucial manner due to the curvature. The interaction of neighboring hydrocarbon chains is still the dominant friction mode, and this friction increases due to the calculated increase in the thickness  $w$  [Eq. (3)].

For a bilayer, the two leaflets have opposite signs of the mean-curvature  $H$ , such that one thins and the other thickens. The lipid diffusion seems to be correlated in both leaflets (entrained motion) [11], and therefore the overall change in the bilayer (both leaflets) thickness will determine the resulting change in the diffusion coefficient. Similarly, the diffusion of a membrane peptide, which penetrates both leaflets, will be determined by the changes to the overall thickness. Note from Eq. (2) that the curvature affects the membrane thickness in an inherently asymmetric way, such that there will always be an overall thickening of the bilayer in the presence of curvature and a consequent reduction in the diffusion. The effect of static curvature on the diffusion in a bilayer is therefore predicted to be weaker (second order) than for the monolayer.

## III. FLUCTUATING CURVATURE

After establishing in Sec. II the applicability of our model to real membranes, we now turn to the effects of curvature fluctuations in an overall flat membrane. The effect of membrane curvature fluctuations on the diffusion coefficient has two contributions: The first comes from the increase in the average membrane thickness, as we discussed above [Eqs. (2) and (3)], and which we shall calculate below. The second is a geometric effect due to the fact that the observed diffusion is a flat projection of the real motion on the undulating surface [4,12]. The first effect will be observed as an effective increase in the intrinsic membrane viscosity [Eq. (1)]:  $\eta_{eff} = \eta w_{eff}/w$ , as probed by local viscosity and fluidity fluorescent indicators [13] and by electron spin resonance (ESR) spectrometry [14]. The sum of both effects (intrinsic and geometric) will be observed by overall diffusion measurements, such as using fluorescence recovery after photobleaching (FRAP) [7,15].

Let us begin with the first effect of increased membrane thickness. The average curvature  $\langle H \rangle$  for each leaflet of the bilayer due to the fluctuations vanishes, as the fluctuations are symmetric. Nevertheless, the curvature fluctuations contribute to the mean-square curvature  $\langle H^2 \rangle$  [Eq. (2)], which

increases the overall membrane thickness. This arises from the inherent asymmetry between the positive and negative curvature undulations; to conserve the volume per molecule the molecules have to increase their length when  $H < 0$ , and decrease it when  $H > 0$ . For  $H$  negative and large the cross section tends to zero, and the molecules lengthen sharply [see Eq. (3) for  $H \rightarrow -1/4w$ ], while for positive  $H$  the molecules thin monotonously.

We will deal with an overall flat membrane, that bends symmetrically in both directions, with  $\langle K \rangle = 0$ ,  $\langle H \rangle = 0$  in Eq. (2). The remaining contribution comes from the mean-square curvature term in Eqs. (1) and (2) due to thermal fluctuations

$$\begin{aligned} \langle w_{eff} \rangle &\approx w(1 + 2w^2 \langle H^2 \rangle) \\ \Rightarrow D &= D_0 \frac{w}{w_{eff}} \approx D_0(1 - 2w^2 \langle H^2 \rangle) \end{aligned} \quad (4)$$

where  $D_0$  is the diffusion coefficient in the flat membrane, and the mean-square curvature is given, for thermal fluctuations, by

$$\langle H^2 \rangle = \frac{1}{(2\pi)^2} \int q^4 \langle h_q^2 \rangle d^2q = \frac{k_B T}{4\pi\kappa w^2} + \frac{k_B T \sigma}{4\pi\kappa^2} \ln\left(\frac{1}{\kappa/\sigma w^2 + 1}\right), \quad (5)$$

where we used [5]:  $\langle h_q^2 \rangle = k_B T / (\kappa q^4 + \sigma q^2)$ , and  $\kappa$ ,  $\sigma$  are the curvature bending modulus and the effective surface tension, respectively. Using Eq. (5) in (4), we get the reduction in the diffusion coefficient

$$D/D_0 \approx 1 - \frac{k_B T}{2\pi\kappa} \left[ 1 + \frac{\sigma w^2}{\kappa} \ln\left(\frac{1}{\kappa/\sigma w^2 + 1}\right) \right]. \quad (6)$$

Note that since the logarithmic term is always negative, increasing the tension will increase the diffusion coefficient, by suppressing the thermal curvature modes that decrease the diffusion coefficient. The surface tension here acts to decrease the average bilayer thickness by flattening the curvature undulations, and not by direct stretching of the flat bilayer, which is much harder to do [5].

The second contribution to the decrease in the effective diffusion due to the membrane fluctuations arises from the increase in the path length of the diffusing particle on the undulating membrane surface [5]. This effect was recently calculated by Reister and Seifert [4]. A simple approximation of this effect follows from noting that the diffusion coefficient is proportional to the membrane area:  $D = \langle r^2 \rangle / t$ , so that the observed diffusion coefficient is now  $D \sim D_0 A_{proj} / A$ , where  $A$  is the real and  $A_{proj}$  is the projected membrane area. The reduction in the diffusion coefficient due to the excess area of membrane fluctuations  $\Delta\alpha = \Delta A / A \approx \int q^2 \langle h_q^2 \rangle d^2q$  [5] is given in the limit of small  $\Delta\alpha$  by

$$D/D_0 = \frac{1}{1 + \Delta\alpha} \approx 1 - \frac{1}{2} \langle (\nabla h)^2 \rangle \approx 1 - \frac{k_B T}{8\pi\kappa} \ln\left(1 + \frac{\kappa}{w^2 \sigma}\right). \quad (7)$$

Note that in all finite systems there is a residual surface tension  $\sigma_0$ , due to surface conservation. In cells this value is

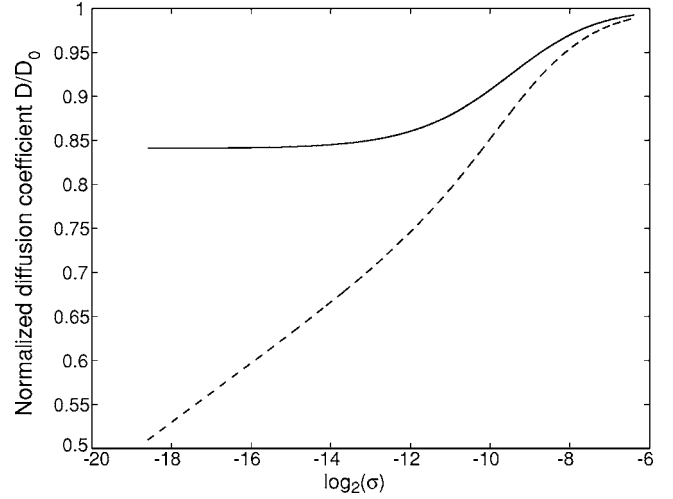


FIG. 2. The calculated dependence of the normalized diffusion coefficient  $D/D_0$  on the effective surface tension  $\sigma$ . To fit the data we use  $\kappa = k_B T$ , bare membrane thickness  $w = 5$  nm, and  $\sigma_0 = k_B T / L^2$ ,  $L = 1 \mu\text{m}$ ; solid line, membrane thickness effect [Eq. (6)]; dashed line, combined thickness and projected area effects [Eqs. (6) and (7)].

usually much larger, determined by the cytoskeleton that is attached to the membrane [16].

In Fig. 2 we plot the calculated reduction in the effective diffusion due to the thickness alone [Eq. (6)], and due to both effects of thermal fluctuations, Eqs. (6) and (7). Note that the “flat” value  $D_0$  increases with temperature, according to Eq. (1), so that the measured value of  $D(T)$  is the combination of both conflicting effects.

Let us note that the calculated increase in the diffusion coefficient  $D$  for increasing surface tension  $\sigma$  [Eqs. (6) and (7)], due to the suppression of the bending modes, could be counter-balanced by the following opposite effect; if the membrane surface tension (and the bending modulus  $\kappa$ ) is increased, for a given fixed geometry, by increasing the strength of the attractive lipid-lipid interactions, then the overall diffusion coefficient decreases due to an increase in  $\eta$  (and decrease in  $D_0$ ). What is shown in Eqs. (6) and (7) is that for a given fixed membrane composition, there will be a gain in diffusion when the surface tension is increased.

#### IV. FLUCTUATING CURVATURE IN ACTIVE MEMBRANES

Finally, we describe the effects of *active* membrane fluctuations [17,18] on the diffusion coefficient. These are membranes which have, in addition to the thermal fluctuations described above, also shape fluctuations that are driven, for example, by chemical energy adenosine triphosphate (ATP). Such membranes arise in living cells [19,20] or in synthetic vesicles, which incorporate ion pumps [18]. The increased amplitude of the membrane fluctuations, compared to the purely thermal contribution, are usually described phenomenologically by introducing a higher effective temperature  $T_{eff} \geq T$  [16,19].

We begin with the case of synthetic active membranes [18], for which several models have been proposed to calcu-

late the active height fluctuations and the consequent  $T_{eff}$  [17,21]. We shall use here a simple model that we previously proposed for such membranes [21], where a uniform density of proteins impart a randomly directed and local impulse of duration  $\tau$ .

Two kinds of proteins were considered: “curvature-force” proteins that actively change their spontaneous curvature, and “direct-force” proteins that impart a normal force to the membrane. The mean-square height fluctuations  $\langle h_q^2 \rangle$  and the excess area for both these cases were calculated in [21]. Since we assume that the thermal and active fluctuations are incoherent, their contributions simply add up to both the mean-square curvature [Eqs. (5) and (6)] and the excess area [Eq. (7)].

For curvature-force active membranes, the excess area behaves as the thermal case [21], adding a thermal-like term to Eq. (7). In such a case it is natural to describe the combined geometrical effect of thermal and active fluctuations on the diffusion using a higher “effective temperature” [18,21]:  $k_B T_{eff} \sim k_B T + 2F^2 n r^4 / \kappa$ , where  $F$  is the active force,  $r$  is the spontaneous curvature of the membrane protein when it is activated, and  $n$  is the areal density of the proteins (assumed to be distributed uniformly). The effect of the active fluctuations on the membrane thickness enters through the contribution to the mean-square curvature [Eq. (5)], which is straightforward to calculate, but gives a lengthy result. For a tension-less membrane we find the following behavior: In the limit of infinitely short bursts ( $\tau \rightarrow 0$ ), the active contribution to the mean-square curvature  $\langle H^2 \rangle_{active,c}$  vanishes. In the limit of static curvature ( $\tau \rightarrow \infty$ ) the result simplifies to  $\langle H^2 \rangle_{active,c} \rightarrow F^2 n r^4 / 16 \pi^2 w^2 \kappa^2$ , which is again thermal-like [Eq. (5)].

Comparing to the experiments we first need to fix the values of the various physical parameters. In the experiments on vesicles containing light-activated bacteriorhodopsin (BR) [18] the excess area was measured by micro pipette aspiration, and it was found that when the BR are activated:  $T_{eff}/T \sim 2-3$  [21]. Comparing to our model, we therefore use this data to fix the value of  $F^2 n r^4 / \kappa \sim k_B T$ . Diffusion experiments on vesicles containing the BR proteins [22] indicate very slow aggregation of the proteins, so we will use the static limit ( $\tau \rightarrow \infty$ ). Using these values we get an active contribution to the thickness effect (6) which amounts to:  $T_{eff}/T \sim 1.25$ . The overall reduction in the diffusion coefficient, due to the BR-induced membrane fluctuations, can be therefore estimated to be  $\sim 15\%$  (using  $\kappa = 10 k_B T$ ,  $\sigma_0 \sim \kappa / L^2$ , and  $L = 10 \mu\text{m}$  [18]).

In the experiments [22], it was found that indeed the diffusion of the BR proteins is reduced by a factor of  $\sim 4$  when they are activated. This large reduction is mainly due to the aggregation of BR proteins, which form complexes  $\sim 3$  times larger than their original radius, such that their diffusion coefficient is reduced according to  $D \propto 1/r \rightarrow \frac{1}{3}$  [23,24]. There remains, therefore, a further reduction of  $\sim 20\%$  in the observed diffusion coefficient when the BR are activated. Our calculated reduction of  $\sim 15\%$  in the diffusion, due to curvature effects, is therefore plausible when compared to the (scant) experimental data. A more exact quantitative comparison is not possible with the available data. A future ob-

servation of the diffusion coefficient of the lipid component in these membranes should be sensitive only to the effects of curvature, and can test our predictions directly.

The second type of active membrane proteins that we previously considered [21] is the “direct-force” kind. The excess area contribution for this case was previously calculated [21]; in the limit of small tension we find that the excess area is given by  $\Delta \alpha_{active,d} \approx (F^2 \tau n / \eta_f \sqrt{\kappa}) \sqrt{1/\sigma}$ . This contribution reduces the diffusion in Eq. (7), in addition to the thermal part. The active contribution to the mean-square curvature is calculated also for the tension-less case:  $\langle H^2 \rangle_{active,d} \sim (F^2 n \tau^{2/3} w^2) / (\kappa^{4/3} \eta_f^{2/3})$ . Using values that we fitted to the experimental data [18,21], we estimate a negligible active contribution of  $\sim 0.1\%$ , to the reduction in the diffusion coefficient.

Note that for this type of active membranes we have a rather curious result: Increasing the viscosity of the surrounding fluid  $\eta_f$  diminishes the amplitude of the active curvature fluctuations [21], and therefore *increases* the diffusion inside the membrane. Of course, this effect is countered by the direct drag of the peptide with the surrounding fluid, which increases with  $\eta_f$  [see the discussion following Eq. (1)].

## V. EFFECT OF SHEAR FLOW ON MEMBRANE DIFFUSION

When shear flow is applied parallel to the surface of a fluid membrane, it results in an increase in the effective surface tension, thereby quenching the height of thermal curvature fluctuations. The setup is of a flow which is parallel to plane of the membrane, with a gradient in the velocity in the direction normal to the plane of the membrane. In the lamellar phase, this increased tension is given by [25]

$$\Delta \sigma \sim \frac{\pi^4}{18} \frac{\kappa d^4}{(k_B T)^2} \eta_f^2 \dot{\gamma}^2, \quad (8)$$

where  $d$  is the lamellar spacing,  $\dot{\gamma}$  is the shear rate, such that the shear stress is:  $\Gamma = \eta_f \dot{\gamma}$ . Using Eq. (8) in (5), we find that in the limit of large shear-rates  $\dot{\gamma} \rightarrow \infty$ , the mean-square curvature due to thermal fluctuations vanish as:  $\langle H^2 \rangle \propto 1/\dot{\gamma}^2$ . The subsequent increase in the diffusion coefficient, according to our calculations, await experiments on membranes in a lamellar phase.

Nevertheless, there are data available from experiments on diffusion in relatively flat cellular membranes [13,15]. In Fig. 3 we compare the calculated shear-induced change in the diffusion coefficient [relative to the value without shear flow  $D(0)$ ] to the experimental data on endothelial cells [13,15]. Note that in the experiments there is no advective effect enhancing the diffusion in the plane of the membrane, which is measured in the perpendicular direction to the flow. In these experiments it was observed that after the application of shear flow there is an initial, fast increase in  $D$ , which we attribute to the induced increase in the membrane tension  $\Delta \sigma$  [Eq. (8)]. The time scale of this initial change in  $D$  is in agreement with the time scale for the onset of the membrane tension, which is of the order  $\tau_{mem} \sim \eta_f L^3 / \kappa \sim 1-5$  sec,



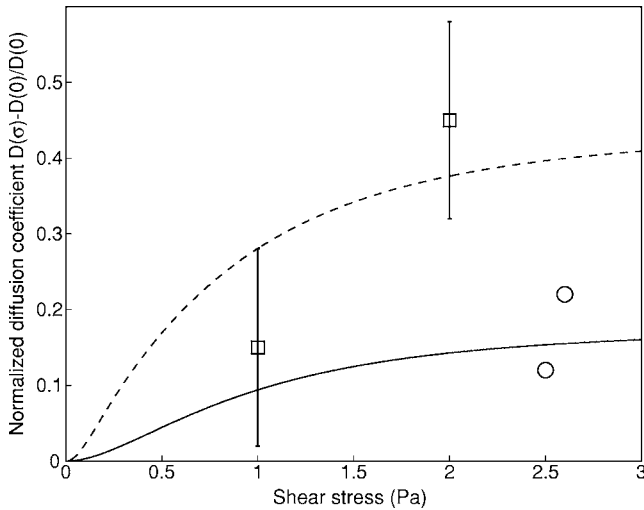


FIG. 3. The calculated change in the normalized diffusion coefficient  $[D(\sigma) - D(0)]/D(0)$ , due to the applied shear stress  $\Gamma = \eta_f \dot{\gamma}$  [Eq. (8)] (using  $\kappa = k_B T$ ,  $d = 100w$ ,  $w = 5$  nm,  $\sigma_0 = k_B T/L^2$ , and  $L = 50$  nm); solid line, membrane thickness effect [Eq. (6)]; dashed line, combined thickness and projected area effect [Eqs. (6) and (7)]. The data points are squares [15]; circles [13].

where  $L \sim 1 \mu\text{m}$  is the order of the cell size [13,15].

To fit to the experimental data [13,15] we used  $d = 500$  nm in Eq. (8). The value of this fitting parameter is reasonable, since it implies that the membrane undulations are confined to  $d/2 \sim 250$  nm by the cytoskeleton that underlies the membrane of these cells [26]. Note that the calculation involving only the changes to the membrane's thickness (viscosity) [Eq. (6)] agrees with the measurements using local viscosity indicators [13] (Fig. 3). The sum of both effects, Eqs. (6) and (7), agrees with the observed changes to the overall diffusion coefficient, using the FRAP method [15]. In these calculations we used  $\kappa/k_B T \sim 1$  in Eqs. (6) and (7). This is reasonable for living cells, since while  $\kappa \sim 5k_B T$ , the amplitude of the active membrane fluctuations are mostly driven by active processes such as actin polymerization and can be phenomenologically described by a higher effective temperature:  $T_{eff}/T \sim 5 - 10$  [19,20] (see the discussion in the previous section). Let us note that due to the limited experimental data we can say that the calculated effect of the increase in membrane tension is merely a possible explanation that is in accord with the experimental observations.

The diffusion coefficient in these cells was observed to further increase over a much longer time scale of  $\sim 100 - 300$  sec, especially at the front (flow-facing) part of the cell [13,15]. The time scale for this change corresponds to the redistribution of membrane proteins through diffusion and advection:  $\tau_{diff} \sim L^2/D \sim 10$  min. Over this longer time-scale the diffusion is seen to change by a large factor of  $\sim 2$ . The shear flow is found to affect the cytoskeleton in various ways [20]; in some cells it reduces the amount of the actin network underlying the membrane [27]. These large-scale changes are usually rather slow compared to hydrodynamic time scales, and can account for the observed slow changes in the diffusion coefficient. These slow processes are beyond the curvature effects we describe here.

Finally let us comment about the effective temperature of the height fluctuations in living cells. A theoretical model describing the active fluctuations of a cell membrane due to actin polymerization was recently proposed [20]. In this model we assume that the actin polymerization that is pushing the membrane is initiated by specific membrane proteins, that are themselves free to diffuse in the membrane. This model therefore couples the dynamics of these proteins in the plane of the membrane, to the driving force of the actin polymerization (assumed here to provide a force purely normal to the membrane). Using this model we find that the actin-driven height fluctuations  $\langle h_q^2 \rangle$  have a thermal-like behavior, but with an effective temperature  $T_{eff}$  that is determined by the various physical parameters of the model. Most notably we find that  $T_{eff} \propto 1/D$ , which results from the following mechanism [20]: large density fluctuations of the membrane proteins drive large variations in the actin pushing force. These variations in the force translate into height fluctuations with an amplitude that depends on the time of their survival, which is itself larger the smaller  $D$  is.

From Eqs. (4)–(6) we find that the diffusion is given:  $D/D_0 \propto 1/(1 + \beta T_{eff}/T)$ , so that we now have  $D/D_0 \propto 1/(1 + \beta D_0/D)$  (neglecting the thermal contribution which is usually much smaller since  $T_{eff}/T \sim 10$ ). We solve this relation and get  $D/D_0 = 1 - \beta$ . The parameter  $\beta$  is a combination of physical parameters of the actin derived motion [20]. This relation for  $D$  means that there is now a critical value  $\beta = 1$  such that  $D$  vanishes. This is a point of instability beyond which there is a runaway process of increase in the amplitude of the active fluctuations and a decrease in  $D$ . At this critical value the active fluctuations diverge which signals an instability of the system (this is a new instability beyond those described in [20]). In reality the divergence is limited by the finite size effects. This behavior is in contrast to thermal fluctuations whose amplitude is independent on  $D$ , and therefore causes  $D$  to vanish only in the limit of  $T \rightarrow \infty$ .

## VI. CONCLUSION

To conclude, we have calculated a different effect of static and fluctuating curvature on the *intrinsic fluidity* of fluid membranes, through curvature-induced changes in the membrane thickness. The resulting description is in good agreement with recent experiments on diffusion in curved fluid monolayers [7]. Our analysis gives a simple explanation for the observed effects of the shear flow on membrane fluidity in living cells, which is an important trigger for cell motility [28]. The predictions concerning the dependence of the diffusion on the membrane tension and curvature fluctuations (thermal and active) can be experimentally tested.

## ACKNOWLEDGMENTS

The author is grateful to Assaf Zemel, Sam Safran, Frank Brown, Yann Gambin, and Wladimir Urbach for many useful discussions. The author is grateful to the EU SoftComp NoE Grant and the Robert Rees Fund for Applied Research for their support.

- [1] P. G. Saffman and M. Delbrück, Proc. Natl. Acad. Sci. U.S.A. **72**, 3111 (1975).
- [2] M. H. Cohen and D. Turnbull, J. Chem. Phys. **31**, 1164 (1959).
- [3] P. F. F. Almeida and W. L. C. Vaz, in *Handbook of Biological Physics*, edited by R. Lipowsky and E. Sackmann (Elsevier Science B.V., New York, 1995).
- [4] E. Reister and U. Seifert, Europhys. Lett. **71**, 859 (2005).
- [5] S. A. Safran, *Statistical Thermodynamics of Surfaces, Interfaces and Membranes*, Frontiers in Physics Vol. 90 (Addison-Wesley, New York, 1994).
- [6] V. N. Paunov, S. I. Sandler, and E. W. Kaler, Langmuir **16**, 8917 (2000).
- [7] Y. Gambin, G. Massiera, L. Ramos, C. Ligoure, and W. Urbach, Phys. Rev. Lett. **94**, 110602 (2005).
- [8] S. May and A. Ben-Shaul, Phys. Chem. Chem. Phys. **2**, 4494 (2000).
- [9] L. Rekvig, B. Hafskjold, and B. Smit, J. Chem. Phys. **120**, 4897 (2004).
- [10] E. Falck, M. Patra, M. Karttunen, M. T. Hyvonen, and I. Vattulainen, Biophys. J. **89**, 745 (2005).
- [11] G. S. Ayton and G. A. Voth, Biophys. J. **87**, 3299 (2004).
- [12] The geometric effect for a static membrane was calculated in J. Balakrishnan, Phys. Rev. E **61**, 4648 (2000).
- [13] M. A. Haidekker, N. L'heureux, and J. A. Frangos, Am. J. Physiol. Heart Circ. Physiol. **278**, H1401 (2000); S. K. Mallipattu, M. A. Haidekker, P. Von Dassow, M. I. Latz, and J. A. Frangos, J. Comp. Physiol., A **188**, 409 (2002).
- [14] J. H. Freed, Annu. Rev. Biophys. Biomol. Struct. **23**, 1 (1994).
- [15] P. J. Butler, G. Norwich, S. Weinbaum, and S. Chien, Am. J. Physiol.: Cell Physiol. **280**, C962 (2001); P. J. Butler, T. C. Tsou, J. Y. Li, S. Usami, and S. Chien, FASEB J. **16**, 216 (2002).
- [16] N. Gov, A. G. Zilman, and S. Safran, Phys. Rev. Lett. **90**, 228101 (2003).
- [17] J.-B. Manneville, P. Bassereau, S. Ramaswamy, and J. Prost, Phys. Rev. E **64**, 021908 (2001); S. Ramaswamy, J. Toner, and J. Prost, Phys. Rev. Lett. **84**, 3494 (2000).
- [18] J.-B. Manneville, P. Bassereau, D. Lévy, and J. Prost, Phys. Rev. Lett. **82**, 4356 (1999); P. Girard, J. Prost, and P. Bassereau, *ibid.* **94**, 088102 (2005).
- [19] N. S. Gov and S. A. Safran, Biophys. J. **88**, 1859 (2005).
- [20] N. Gov and A. Gopinathan, Biophys. J. **90**, 454 (2006).
- [21] N. Gov, Phys. Rev. Lett. **93**, 268104 (2004).
- [22] N. Kahya, D. A. Wiersma, B. Poolman, and D. Hoekstra, J. Biol. Chem. **277**, 39304 (2002).
- [23] Y. Gambin, R. Lopez-Esparza, M. Reffay, E. Sierecki, N. S. Gov, M. Genest, R. S. Hodges, and W. Urbach, Proc. Natl. Acad. Sci. U.S.A. **103**, 2098 (2006).
- [24] See a similar behavior also in C. C. Lee and N. O. Petersen, Biophys. J. **84**, 1756 (2003).
- [25] A. G. Zilman and R. Granek, Eur. Phys. J. B **11**, 593 (1999).
- [26] M. Bailly, F. Macaluso, M. Cammer, A. Chan, J. E. Segall, and J. S. Condeelis, J. Cell Biol. **145**, 331 (1999).
- [27] H. Q. Chen, W. Tian, Y. S. Chen, L. Li, J. Raum, and K.-L. Paul Sung, Biorheology **41**, 655 (2004).
- [28] I. Lavelin and B. Geiger, J. Biol. Chem. **280**, 7178 (2004); M. L. Albuquerque and A. S. Flozak, J. Cell Physiol. **195**, 50 (2003).